MDPI

Article

Bacterial Community Characteristics and Roles in Nitrogen Transformation in Industrial Farming Systems of *Litopenaeus vannamei*

Hongwei Shan [1], Yulong Du [1], Tao Li [3], Fang Wang [1], Hongyu Li [3] and Haitao Wang [2,*]

1 The Key Laboratory of Mariculture (Ocean University of China), Ministry of Education, Qingdao 266003, China; shanhongwei@ouc.edu.cn (H.S.); duyulong@stu.ouc.edu.cn (Y.D.); wangfang249@ouc.edu.cn (F.W.)
2 Weihai Wendeng District Marine Development Affairs Center, Weihai 264400, China
3 Guang Dong Haid Group Co., Ltd., Guangzhou 511400, China; lit21@haid.com.cn (T.L.); lihy@haid.com.cn (H.L.)
* Correspondence: 3306245@163.com; Tel.: +86-532-82031912

Abstract: Industrial farming is one of the main farming systems used for *L. vannamei*, and it is also the main direction of development in the future. To investigate the role of the bacterial community in nitrogen transformation in industrial *L. vannamei* farming systems, we studied the concentration of nitrogen compounds, the bacterial community using 16S rRNA sequencing, and nitrogen cycling genes' abundance using absolute quantitative PCR in aquaculture water (using seawater (WD) and groundwater mixed with seawater (CY)) and analyzed the correlations between them using a person analysis. The results showed that the bacterial α-diversity index (ACE, Shannon, and Sobs) significantly changed during culture in WD but not in CY. Bacterial community species composition analysis and linear discriminant analysis effect size (LEfSe analysis) revealed that *Cyanobiaceae* and *Microbacteriaceae* were the dominant bacteria and biomarkers in WD. *Vibrionaceae*, *Ateromonadaceae*, *Microbacteriaceae*, *Saprospiraceae*, and *Cryomorphaceae* were the dominant bacteria and biomarkers in CY. A functional annotation of procaryotic taxa (FAPROTAX) analysis revealed that the bacterial community in WD exhibited a greater phototrophic activity at early culture stages, while at the same stage, CY exhibited strong nitrate reduction. A correlation analysis of nitrogen cycling genes and environmental factors revealed that *napA*, *narG*, *ureC*, *amoA*, and *nirK* were significantly correlated with the concentrations of total ammonia nitrogen (TAN), nitrite (NO_2^--N), nitrate (NO_3^--N), and total nitrogen (TN) in WD. In CY, *amoA* was positively correlated and *napA* and *nirK* were negatively correlated with TAN and TN concentrations. A correlation analysis between bacterial abundance and environmental factors revealed that *Flavobacteriaceae*, *Saprospiraceae*, *Cryomorphaceae*, *Cyanobiaceae*, *Halieaceae*, and *Cyclobacteriaceae* were significantly correlated with the concentrations of TAN and NO_2^--N. The above results indicated that the bacterial community in industrial shrimp farming systems changed under different conditions, with consequent changes in the abundance of genes being involved in the nitrogen cycle and in this biogeochemical process in the water. Our study facilitates further understanding of microbes and their functions in nitrogen cycling in industrial shrimp farming systems.

Keywords: *Litopenaeus vannamei*; industrial farming systems; bacterial community; nitrogen cycling genes

1. Introduction

In recent years, the aquaculture industry has flourished, which greatly alleviates the current problem of human protein requirements worldwide. *Litopenaeus vannamei* is the most farmed crustacean globally because of its high meat yield, strong stress resistance, excellent adaptability to salinity, and low dietary protein. According to farming data provided by the FAO, the worldwide production of *L. vannamei* in 2020 accounted for 51.7% of the total crustacean production worldwide [1]. In China, *L. vannamei* is cultured in

a variety of models, including industrial farming, higher-place ponds farming, outdoor ponds farming, and shed farming [2]. Among these models, industrial farming is a very popular farming system that has the advantages of a standardized culture process, high culture density, and high output, and it has become one of the most important farming systems in North China.

In highly intensive industrial farming systems, residual feed and accumulated feces can settle in the middle and lower layers of the water. These substances are rich in proteins and other organic matter and are decomposed by heterotrophic bacteria, increasing the concentration of nitrogen compounds in the water [3]. TAN refers to nitrogen-containing compounds in the form of free ammonia (NH_3) and ammonium ions (NH_4^+), which is a toxic nitrogen-containing pollutant in aquaculture water; excessive ammonia nitrogen destroys gill tissue [4,5], affects the transport and metabolism of substances, reduces immunity [6], and increases susceptibility to disease in aquaculture animals [7,8]. Nitrite is another major pollutant in aquaculture water that can damage the granular and semi-granular hemocytes of aquaculture organisms [9,10]. For crustaceans that rely primarily on hemolymph for nonspecific immunity, damage to blood cells often results in reduced immunity and an increased likelihood of death [11].

The transformation of many organic compounds in water is performed thanks to microorganisms [12]. The composition and abundance of these microbes are related to environmental factors, such as temperature [13], dissolved oxygen (DO) [14], and salinity [15], especially the processes of the nitrogen cycle in water, which are mostly carried out by microbes [16]. For example, cyanobacteria can fix nitrogen by immobilizing N_2 from the air to ammonia nitrogen for bioenergy use [17]. *Mycobacterium tuberculosis* is involved in assimilatory nitrate reduction and in ultimately converting nitrate into bacterial proteins [18]. *Saprospiraceae* is related to nitrate removal by denitrification in aquaculture water [19]. Therefore, to explore the pathway and mechanism underlying nitrogen transformation, identifying the composition and changes in microbes is necessary.

Although microbes play a crucial role in nitrogen transformation in aquaculture systems, relevant research data are still lacking with respect to industrial farming systems. Therefore, in this study, we sampled two industrial farming systems with different water sources; determined the water environmental factors, bacterial community characteristics, and abundances of nitrogen cycling genes in bacterial communities; and conducted a correlation analysis to (1) characterize bacterial communities in cultured water and their succession characteristics, (2) determine relationships between nitrogen cycling genes and environmental factors, and (3) reveal correlations between bacterial abundances and environmental factors. Our study will facilitate further understanding of microbes and their role in nitrogen cycling in the industrial shrimp farming and provide theoretical support for solving the problem of harmful nitrogen compound accumulation through bacterial regulation.

2. Materials and Methods

All experimental procedures were performed following the regulations of the People's Republic of China on the Administration of Laboratory Animals (http://www.gov.cn/gongbao/content/2011/content_1860757.htm, accessed on 1 September 2022).

2.1. Collection of Water and Shrimp Samples

The sampled industrial *L. vannamei* farming companies in this study were located in Wendeng District, Weihai city, Shandong Province (36.92° N, 122.07° E; hereafter referred to as WD), and Changyi District, Weifang city, Shandong Province (37.05° N, 119.50° E; hereafter referred to as CY). The geographical information of the above two sampling companies is shown in Figure 1. From July to September 2022, 4 ponds were selected for sampling in WD and CY. Water samples were collected in the 1st, 3rd, 5th, 7th, and 9th weeks of shrimp culture and labeled as WD1, WD3, WD5, WD7, and WD9, and CY1, CY3, CY5, CY7, and CY9, respectively.
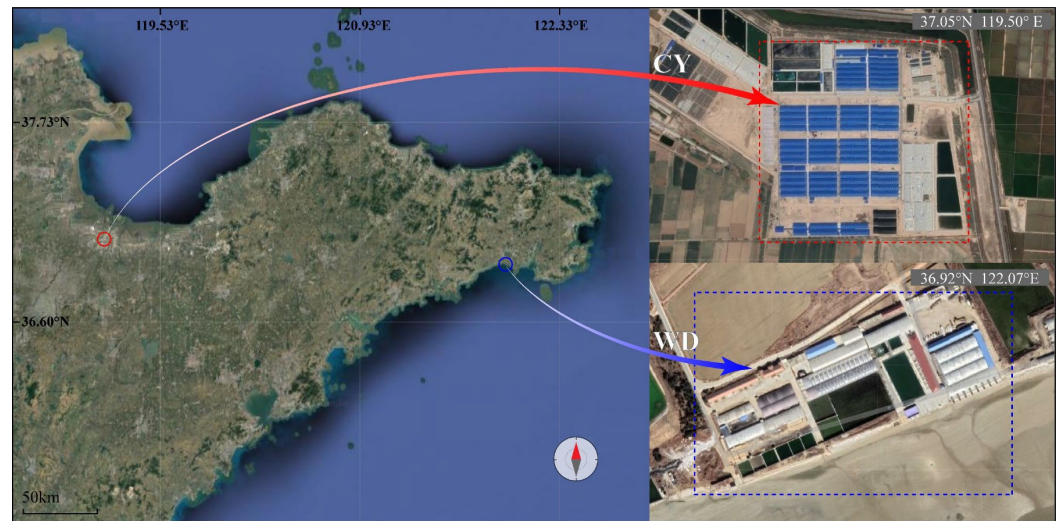
Figure 1. The locations of the sampling sites were Wendeng District, Weihai city, Shandong Province (36.92° N, 122.07° E), and Changyi District, Weifang city, Shandong Province (37.05° N, 119.50° E).

One liter of water sample was filtered with sterilized mixed-fiber filter membranes (0.22 μm, Shanghai Lichen Bangxi Instrument Technology Co., Ltd., LC-95WD, Shanghai, China) after being collected from each sampling pond. The filtered water was transported back to the laboratory and stored at −20 °C immediately for the determination of the concentrations of total ammonia nitrogen (TAN), nitrite nitrogen (NO_2^--N), nitrate nitrogen (NO_3^--N), and total nitrogen (TN). The membrane was loaded into a sterilized freezer tube, frozen with liquid nitrogen, and then stored at −80 °C for DNA extraction. The biological length of the cultured shrimp at the same sampling time is shown in Figure S1, and no significant difference was found in shrimp lengths between the two sampling sites at the same time.

2.2. Determination of Physical and Chemical Indices of Water

A thermometer was used to determine the water temperature. A pH meter (Shanghai Lichen Instrument Equipment Co., Ltd., LC-pH-100B, Shanghai, China) was used to determine the water pH. A diopter salinometer (Guangzhou Suwei Electronic Technology Co., Ltd., LS10T, Guangzhou, China) was used to determine the water salinity. A dissolved oxygen (DO) meter (Changchun Leprotactinium Technology Co., Ltd., AZ8403, Changchun, China) was used to determine the DO concentration in the water. The concentration of TAN, NO_2^--N, NO_3^--N, and TN were determined, following the methods of Chen et al. [20].

2.3. Extraction of 16S rDNA from Bacterial Samples and Illumina Sequencing

DNA was extracted from the water filter membrane with a FastDNA® SPIN kit (MP BiomeDicals, Santa Ana, CA, USA), following the manufacturer's instructions. After extraction, the concentration and purity of the extracted DNA were determined by a NanoDrop ND2000 (USA), and the integrity of the extracted genomic DNA was assessed by 1% agarose gel electrophoresis. The V3–V4 variable region of the bacterial 16S rRNA was amplified with primers 338F (5′-ACTCCTACGGGAGGCAGCAG-3′) and 806R (5′-ACTCCTACGGGAGGCAGCAG-3′). Then, the amplification products were sent to Shanghai Meiji Biomedical Technology Co., Ltd. (Shanghai, China) for second-generation sequencing using the Illumina MiSeq PE 300 platform.

The original bacterial 16S rRNA sequencing data have been uploaded to the NCBI database, and the accession number is PRJNA1052999. Fastp (https://github.com/OpenGene/Fastp, accessed on 3 January 2023) was used for quality control of the original sequence. Flash (https://ccb.jhu.edu/software/FLASH/index.shtml, accessed on 3 January 2023) was used for paired-end double-end sequence splicing. Usearch (http://www.drive5.com/usearch/, accessed on 3 January 2023) was used for OTU statistical analysis. Uparse

(http://www.drive5.com/uparse/, accessed on 3 January 2023) was used to cluster OTU sequences based on similarity (97%). The RDP classifier (https://sourceforge.net/projects/rdp-classifier/, accessed on 3 January 2023) was used for sequence classification annotation. Species classifications were compared with the SILVA138/16s_bacteria database, and the classification confidence was 0.7.

2.4. Absolute Quantitative Determination of Nitrogen Cycling Genes

The absolute abundances of the *napA*, *nirK*, *nirS*, *ureC*, *amoA*, *narG*, and *nxrB* genes in the WD and CY groups were determined via real-time quantitative PCR. The primer sequences used for PCR are shown in Table 1.

Table 1. The primers and their sequences used in this study.

Genes	Sequences of the Primers (5′→3′)	References
napA	(F) TGGACVATGGGYTTYAAYC	[21]
	(R) CCTTCYTTYTCSACCCACAT	[22]
nirK	(F) ATCATGGTSCTGCCGCG	[22]
	(R) GCYTCGATCAGRTTRTGGTT	[22]
nirS	(F) GTSAACGTSAAGGARACSGG	[21]
	(R) GASTTCGGRTGSGTCTTGA	[22]
ureC	(F) AARMTSCAYGARGACTGGGG	[22]
	(R) TGRCASACCATSAKCATGTC	[22]
amoA	(F) GGHGACTGGGAYTTCTGG	[23]
	(R) CCTCKGSAAAGCCTTCTTC	[23]
narG	(F) ACSCAYGGSGTWDAACTGYAC	[21]
	(R) GGNACGTTNGASCCCCA	[24]
nxrB	(F) GTGGAACAAYGTGGARACSAAGCC	[25]
	(R) CGGTTCTGGTCRATCA	[26]

Note: The letters in the primers other than ACTG represent the abbreviated bases, as shown in Table S1.

The target gene was amplified using SYBR Green qPCR with a ChamQ SYBR Color qPCR MasterMix (High ROX Premixed) kit (Noweizan, Nanjing, China), following the manufacturer's instructions. A StepOne Plus Real-Time PCR system (Waltham, MA, USA) was used for the experiment, and every gene holds three technical replicates in each sample. The reaction system was 10 μL, in which the fluorescence reagent (2× ChamQ SYBR Color qPCR Master Mix (High ROX Premixed)) was 5μL, the template DNA was 2 μL, forward and reverse primers were 0.2 μL, respectively, and DEPC H_2O was 2.6 μL. The PCR reaction procedure is as follows: pre-denaturation at 95 °C for 20 s; 40 cycles, each consisting of 95 °C for 3 s and 60 °C for 30 s.

The primers and sample DNA were also sent to Shanghai Meiji Biomedical Technology Co., Ltd. (Shanghai, China) to construct a standard plasmid. The standard plasmid was diluted, and a standard curve ($R^2 > 0.99$) was constructed. DEPC H_2O was used as the template for the negative control, and no primer dimer crest was found.

2.5. Data Analysis

The original sequences were subjected to quality control, splicing, OTU statistical analysis, sequence annotation, and species classification, and Mothur software (https://www.mothur.org/wiki/download_mothur, version 1.30.2, accessed on 3 January 2023) was used to calculate the α-diversity indices (Sobs, Shannon, Ace). R version 3.3.1 was used for community species composition analysis, β-diversity analysis (principal coordinates analysis (PCoA)), intergroup diversity analysis, and environmental factor correlation analysis (Pearson). Linear discriminant analysis (LDA) was performed based on the taxonomic composition using LEfSe software (http://huttenhower.sph.harvard.edu/LEfSe, version 1.0, accessed on 3 January 2023). The functional prediction of bacterial communities was performed using the FAPROTAX database. The β-diversity distance matrix was calculated using QIIME (http://qiime.org/install/index.html, version 1.9.1, accessed on 3 January 2023), and the

differences between groups were tested using the ANOSIM method. The Kruskal-Wallis rank sum test was used to analyze the significance of differences for each group. $p < 0.05$ was considered as a threshold value to indicate a significant difference.

All data are presented in the form of mean ± standard deviation for each group. SPSS 26.0 software was used to test the significance of the differences of the data in this study. For normally distributed data, we chose a one-way ANOVA to test the significance; if the data conformed to the homogeneity of variance, Tukey's test was used for post hoc comparisons; otherwise, Tamhane's T2 test was used. If there was a significant, the nonparametric test and Kruskal-Wallis H test were used. There is a significant difference between the corresponding data when $p < 0.05$.

3. Results

3.1. Physical and Chemical Measurements

As shown in Table S2, during the sampling, the water temperature in the WD group was 28.1 ± 1.98 °C, the salinity was 29–30, the pH was 7.66 ± 0.29, and the dissolved oxygen concentration was 5.76 ± 0.60 mg/L. In the CY group, the water temperature was 28.5 ± 0.73 °C, the salinity was 25–26, the pH was 7.98 ± 0.18, and the dissolved oxygen concentration was 5.74 ± 0.20 mg/L.

3.2. α-Diversity of Bacterial Community

The ACE, Shannon, and Sobs indices of the water bacterial community in the WD group are shown in Figure 2a–c. With the progression of culture, the ACE index first increased and then decreased. The maximum ACE index was observed in WD7, which was significantly greater than that in WD1, WD3, and WD9. The lowest ACE index was observed in WD1 and was significantly lower than that in WD3, WD5, and WD7 ($p < 0.05$). The Shannon index first increased and then remained stable and was significantly greater in WD3 and WD7 than in WD1 ($p < 0.05$). The Sobs index first increased and then decreased, and it was significantly greater in WD5 and WD7 than in WD1 and WD9 ($p < 0.05$).
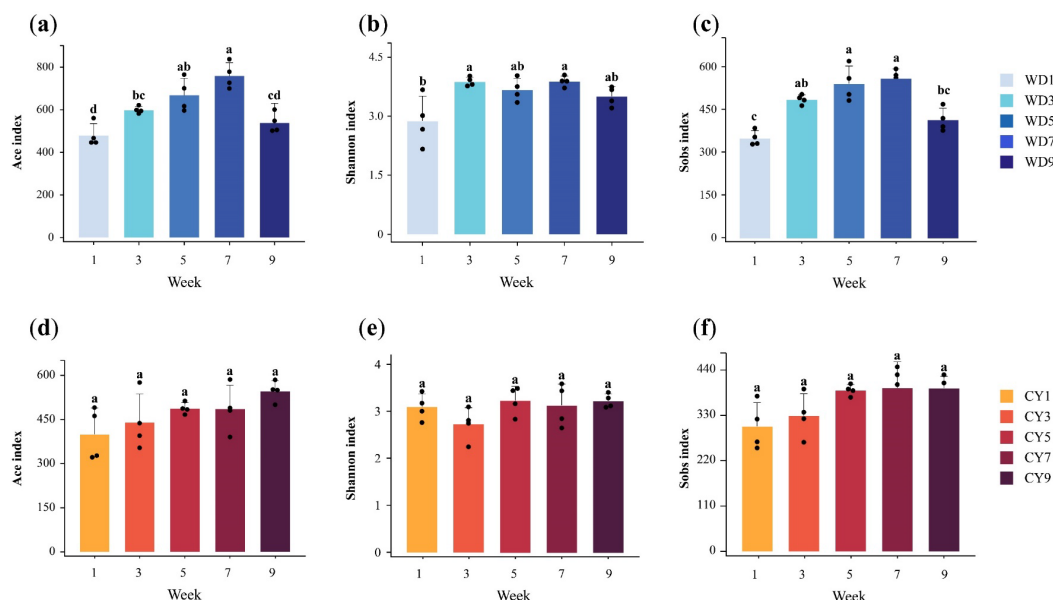
Figure 2. The α-diversity indices of the water bacterial communities in WD and CY. (**a**–**c**) are the ACE, Shannon, and Sobs indices of WD, respectively. (**d**–**f**) are the ACE, Shannon, and Sobs indices of CY, respectively. Note: Different superscript letters within the same group indicate significant differences between groups ($p < 0.05$); Dots in the figure are the values of the replicates for each group.

The ACE, Shannon, and Sobs indices of the water bacterial community in the CY group are shown in Figure 2d–f. The ACE and Sobs indices gradually increased with

increasing culture time. The Shannon index was low only in the CY3 samples and remained unchanged at other times. There were no significant differences in the three indices during the culture period ($p > 0.05$).

3.3. β-Diversity of Bacterial Community

Figure 3a shows the results of the PCoA analysis of the water bacterial community in the WD group. The ANOSIM test yielded $R^2 = 0.6033$, and $p = 0.001$ means significant differences in bacterial communities during the culture period. Figure 3b shows the results of the PCoA analysis of the water bacterial community in the CY group. The ANOSIM test yielded $R^2 = 0.5850$, and $p = 0.001$ means significant differences in bacterial communities during the culture period.
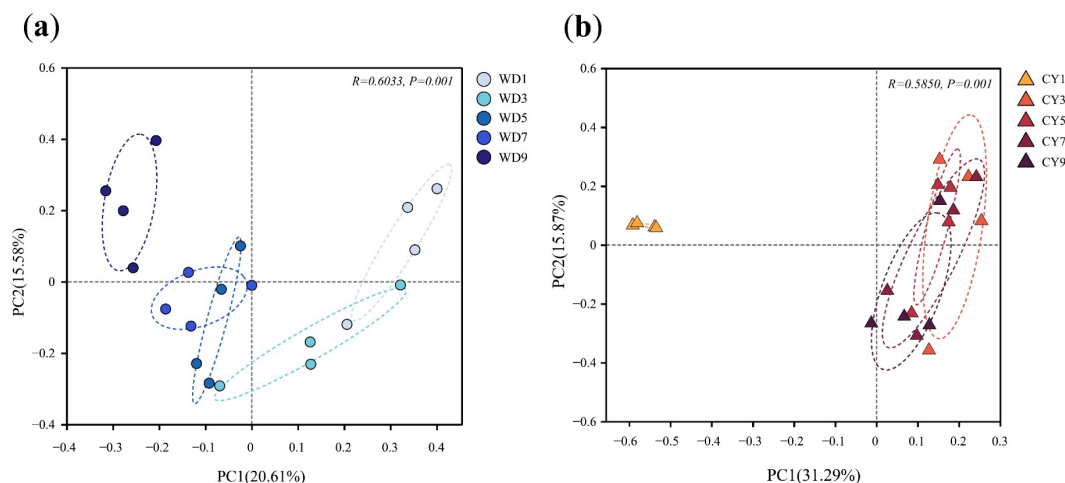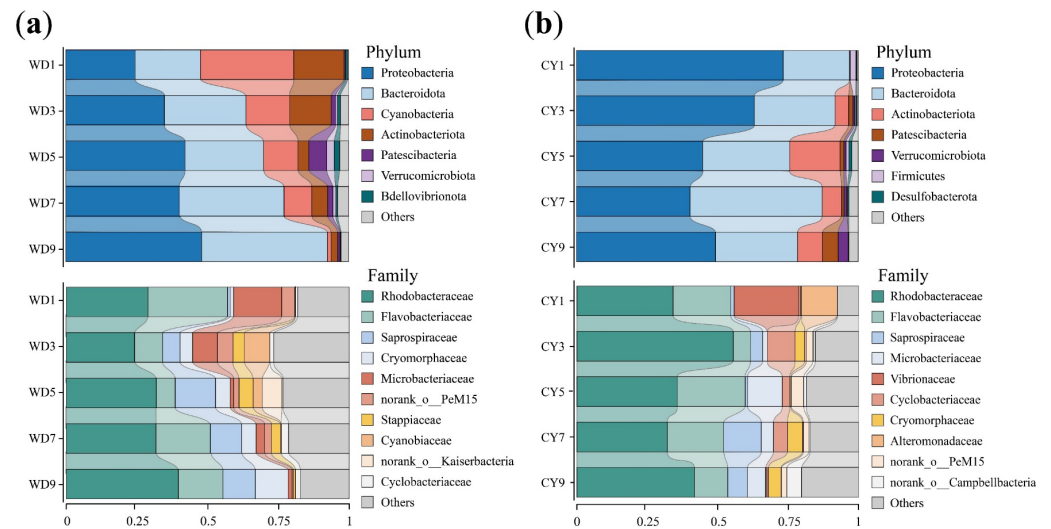

Figure 3. PCoA analysis of bacterial communities in WD (**a**) and CY (**b**) at the OTU level.

3.4. Composition of the Bacterial Community

The composition of the bacterial community in the WD group at the phylum level and family level is shown in Figure 4a. The dominant phyla in the WD group included Proteobacteria, Bacteroidetes, cyanobacteria, Actinobacteria, Patescibacteria, Verrucomicrobiota, and Bdellovibrionota. With the progression of culture, the relative abundances of *Rhodobacteraceae*, *Cryomorphaceae*, and *Saprospiraceae* increased, while those of *norank_o_PeM15* and *Microbacteriaceae* gradually decreased. The abundance of *Flavobacteriaceae* tended to decrease first and then increase, while those of *Stappiaceae*, *Cyanobiaceae*, and *Cyclobacteriaceae* showed the opposite trend.

The composition of the bacterial community of the CY group at the phylum level and family level is shown in Figure 4b. The dominant bacteria in the CY group included Proteobacteria, Bacteroidetes, Actinobacteria, Patescibacteria, and Verrucomicrobiota. With the progression of culture, the relative abundance of *Rhodobacteraceae* first increased and then remained stable. *Flavobacteriaceae* first decreased and then remained stable. The relative abundances of *Saprospiraceae*, *Microbacteriaceae*, and *Cryomorphaceae* tended to gradually increase, while that of *Cyclobacteriaceae* first increased and then decreased. The relative abundances of *Vibrionaceae* and *Alteromonadaceae* were high in CY1 at 22.83% and 12.84%, respectively, but decreased and subsequently remained at a low level.

Figure 4. Bacterial composition at the phylum and family levels in the WD (**a**) and CY (**b**) groups.

3.5. LEfSe Analysis of Bacterial Community Species Composition

The LEfSe analysis of the bacterial community in the WD group is shown in Figure 5a. The biomarkers of WD1 were *Microbacteriaceae*, *Llumatobacteraceae*, Microtrichales, *Balneolaceae*, and Actinobacteria. The biomarkers of WD3 were *Cyanobiaceae*, Synechococcales, PeM15, and Rhodothermia. The biomarkers of WD5 were *Stappiaceae*, *Rubritalaceae*, and Verrucobacteriales. The biomarkers of WD9 were Chitinophagales and *Pseudoalteromonadaceae*.
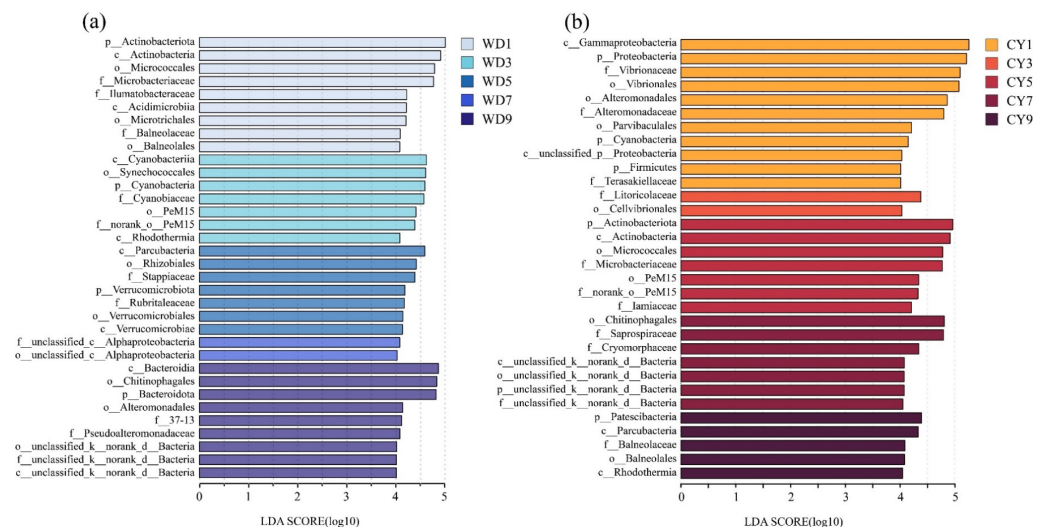
Figure 5. LEfSe analysis of bacterial communities in the WD (**a**) and CY (**b**) groups.

The LEfSe analysis of the bacterial community in the CY group is shown in Figure 5b. The biomarkers of CY1 were Gammaproteobacteria, *Vibrionaceae*, *Ateromonadaceae*, Parvibaculale, cyanobacteria, Firmicutes, and Terasakiellaceae. The biomarkers of CY3 were *Litoricolaceae* and Cellvibrionales; those of CY5 were *Microbacteriaceae*, PeM15, and Iamiaceae; those of CY7 were *Saprospiraceae* and *Cryomorphaceae*; and those of CY9 were *Balneolaceae* and Rhodothermia.

3.6. Difference Analysis of Bacterial Community

The comparative analysis of bacterial community in the WD group at different sampling times (family level) is shown in Figure 6a. There were significant differences in the relative abundances of *Microbacteriaceae* and *norank_o_PeM15* at different sampling times. *Microbacteriaceae* in WD1 and WD3 were significantly higher than that in WD5,

and *norank_o_PeM15* in WD9 was significantly lower than that in other groups ($p < 0.05$). Figure 6b shows the difference analyses of the bacterial community in the CY group at different sampling times (family level). The abundances of *Vibrionaceae* and *Alteromonadaceae* in CY1 were significantly higher than those in the other four groups, and *Saprospiraceae* in CY7 was significantly higher than that in CY5 ($p < 0.05$).

(a)

(b)
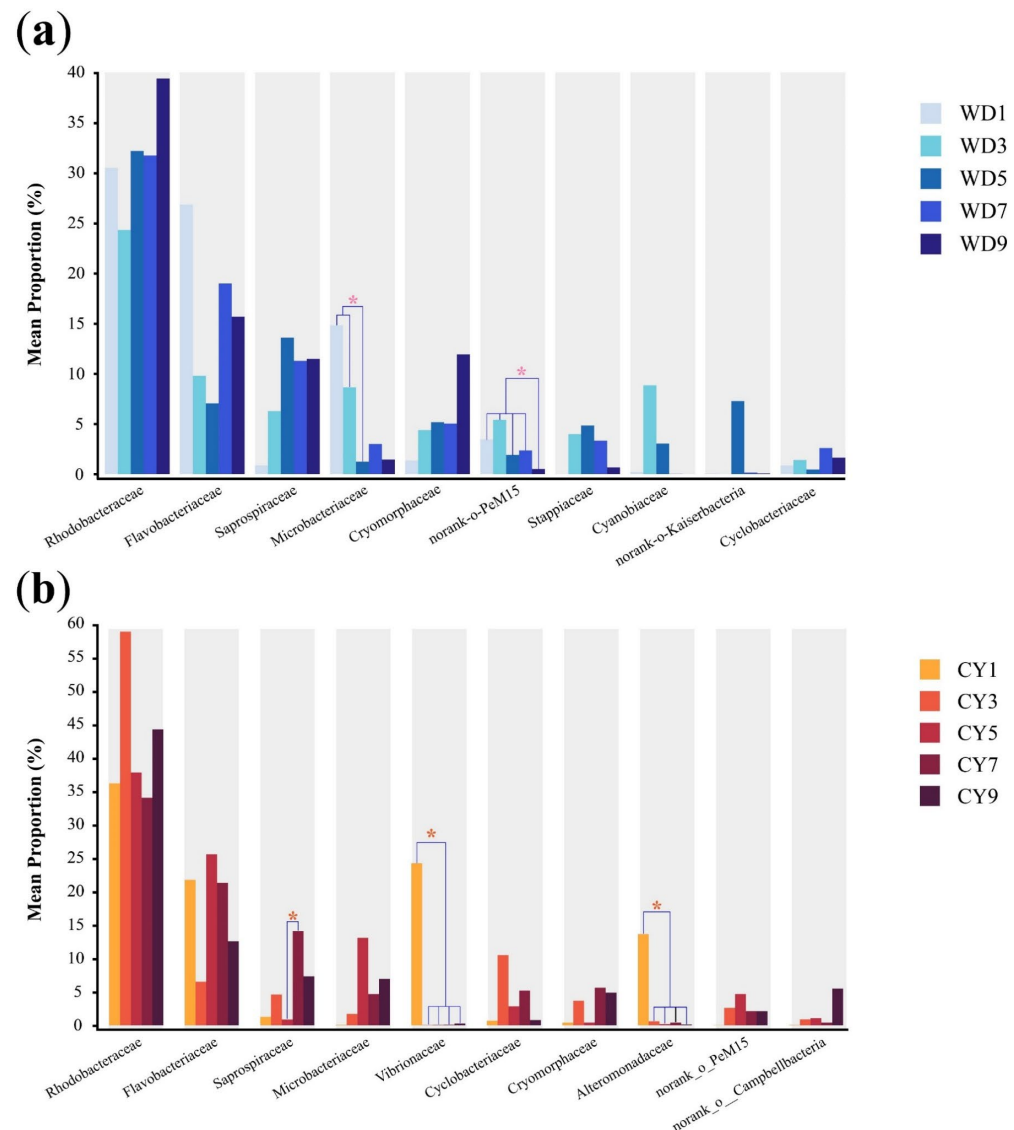
Figure 6. Difference analysis of bacterial communities in the WD group (**a**) and CY group (**b**) at the family level. Note: "*" means there is a significant difference between the groups.

3.7. Functional Prediction Analysis of Bacterial Community

Figure 7 shows the results of the FAPROTAX functional prediction analysis of bacterial communities in the WD and CY groups. The results showed that chemoheterotrophy had the highest abundance both in WD and CY, and phototrophs' abundance in the WD group was higher than that of CY. The abundance of phototrophs in the WD group increased from WD1 to WD5 but remained high only in WD3 and WD5. However, it remained low throughout the whole culture process in the CY group. In addition, the abundance of nitrate reduction function first decreased and then increased in the WD group, while there was a decreasing trend in the CY group. At CY1, all nitrogen reduction functions, including nitrogen respiration, nitrate respiration, nitrite respiration, and nitrate/nitrite/nitrous oxide denitrification in the CY group were higher than those in WD.
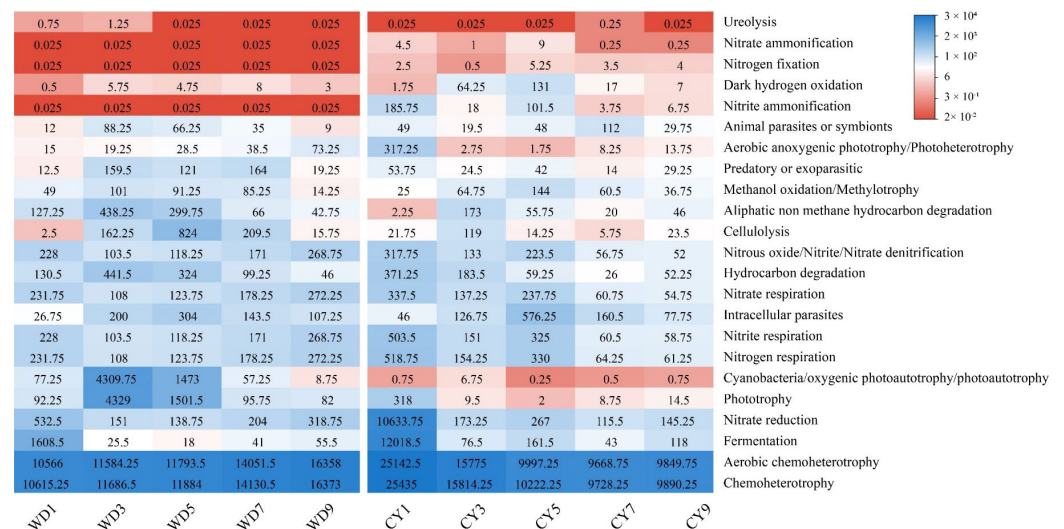
WD1	WD3	WD5	WD7	WD9	CY1	CY3	CY5	CY7	CY9	
0.75	1.25	0.025	0.025	0.025	0.025	0.025	0.025	0.25	0.025	Ureolysis
0.025	0.025	0.025	0.025	0.025	4.5	1	9	0.25	0.25	Nitrate ammonification
0.025	0.025	0.025	0.025	0.025	2.5	0.5	5.25	3.5	4	Nitrogen fixation
0.5	5.75	4.75	8	3	1.75	64.25	131	17	7	Dark hydrogen oxidation
0.025	0.025	0.025	0.025	0.025	185.75	18	101.5	3.75	6.75	Nitrite ammonification
12	88.25	66.25	35	9	49	19.5	48	112	29.75	Animal parasites or symbionts
15	19.25	28.5	38.5	73.25	317.25	2.75	1.75	8.25	13.75	Aerobic anoxygenic phototrophy/Photoheterotrophy
12.5	159.5	121	164	19.25	53.75	24.5	42	14	29.25	Predatory or exoparasitic
49	101	91.25	85.25	14.25	25	64.75	144	60.5	36.75	Methanol oxidation/Methylotrophy
127.25	438.25	299.75	66	42.75	2.25	173	55.75	20	46	Aliphatic non methane hydrocarbon degradation
2.5	162.25	824	209.5	15.75	21.75	119	14.25	5.75	23.5	Cellulolysis
228	103.5	118.25	171	268.75	317.75	133	223.5	56.75	52	Nitrous oxide/Nitrite/Nitrate denitrification
130.5	441.5	324	99.25	46	371.25	183.5	59.25	26	52.25	Hydrocarbon degradation
231.75	108	123.75	178.25	272.25	337.5	137.25	237.75	60.75	54.75	Nitrate respiration
26.75	200	304	143.5	107.25	46	126.75	576.25	160.5	77.25	Intracellular parasites
228	103.5	118.25	171	268.75	503.5	151	325	60.5	58.75	Nitrite respiration
231.75	108	123.75	178.25	272.25	518.75	154.25	330	64.25	61.25	Nitrogen respiration
77.25	4309.75	1473	57.25	8.75	0.75	6.75	0.25	0.5	0.75	Cyanobacteria/oxygenic photoautotrophy/photoautotrophy
92.25	4329	1501.5	95.75	82	318	9.5	2	8.75	14.5	Phototrophy
532.5	151	138.75	204	318.75	10633.75	173.25	267	115.5	145.25	Nitrate reduction
1608.5	25.5	18	41	55.5	12018.5	76.5	161.5	43	118	Fermentation
10566	11584.25	11793.5	14051.5	16358	25142.5	15775	9997.25	9668.25	9849.75	Aerobic chemoheterotrophy
10615.25	11686.5	11884	14130.5	16373	25435	15814.25	10222.25	9728.25	9890.25	Chemoheterotrophy

Color scale: 3×10^4, 2×10^3, 1×10^2, 6, 3×10^1, 2×10^2

Figure 7. Predictive analysis of the functions of the WD and CY bacterial communities.

3.8. Changes in Functional Genes

The changes in the abundances of the denitrification genes *nirS*, *narG,* and *nirK* in the WD and CY groups are shown in Figure 8a–c. With the progression of culture, the abundance of *nirS* gene in the CY group showed a degreasing trend, and the trend was 2.2×10^5~9.8×10^5 copies/mL. The abundance of *nirS* in the CY group showed a decreasing trend, and they were significantly lower in CY5 and CY7 than those in the samples from other weeks ($p < 0.05$). *nirS* in the CY group was always higher than that in WD. The abundance of *nirK* genes in the WD and CY groups first decreased and then increased. The lowest value was found in WD7 in WD, which was significantly lower than that in WD1 and WD9 ($p < 0.05$). No significant difference was found in *nirK* abundance among the CY samples ($p > 0.05$). The abundances of the *narG* gene in the WD and CY groups showed an increasing trend, and the abundances between the two groups were similar. In the WD group, the abundances in WD7 and WD9 were significantly higher than those in the other weeks, and the abundance in WD3 was also significantly higher than that in WD5. In the CY group, the abundance of *narG* in CY9 was significantly higher than that in CY1 and CY5, and that in CY7 was also significantly higher than that in CY1 ($p < 0.05$).

The changes in the dissimilatory nitrate reduction to ammonium (DNRA) gene *napA* in the WD and CY groups are shown in Figure 8d. The abundance of *napA* in the WD group increased, and that in WD9 was significantly higher than that in other weeks ($p < 0.05$). *napA* in the CY group showed a decreasing trend, and it was highest in CY1, which was significantly higher than that in the other weeks ($p < 0.05$).

The changes in the nitrification genes *amoA* and *nxrB* in the WD and CY groups are shown in Figure 8e,f, respectively. *amoA*'s abundance in both the WD and CY groups showed an increasing trend, and the lowest abundance appeared in CY5. In WD, the abundance in WD9 was significantly greater than that in WD3, WD5, and WD7, and the abundances in WD3 and WD7 were also significantly greater than that in WD5. In CY, its abundance in CY9 was significantly greater than in the other weeks ($p < 0.05$). The abundance of the *nxrB* gene in the WD group was low, the variation range was small, and the highest abundance was only 2.8×10^4 copies/mL. *nxrB* in the CY group showed an increasing trend, and the highest abundance was observed in CY9, which was significantly higher than that in CY1 ($p < 0.05$).

The changes in the ammonification gene *ureC* in the WD and CY groups are shown in Figure 8g. *ureC*'s abundance in the WD group increased gradually and reached the highest level in WD9, which was significantly greater than that in the other samples. In CY, it first increased and then decreased. Its abundance in CY3 was significantly higher than in the other samples ($p < 0.05$).
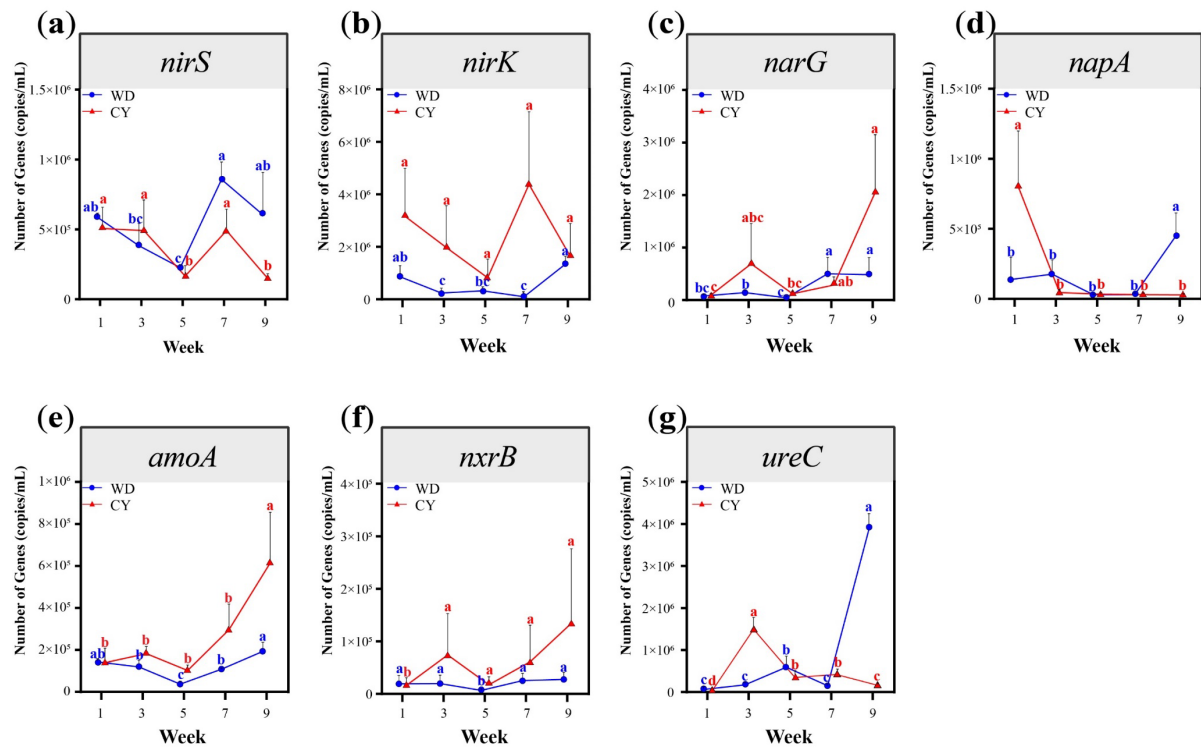
Figure 8. Changes in the abundance of nitrogen cycling genes. (**a**): nirS; (**b**): nirK; (**c**): narG; (**d**): napA; (**e**): amoA; (**f**): nxrB; (**g**): ureC. Different letters with the same color indicate significant differences in the group ($p < 0.05$).

3.9. Correlation Analysis between Nitrogen Cycling Genes and Environmental Factors

The correlation analysis of nitrogen cycling genes and environmental factors in the WD group is shown in Table 2. The TAN, NO_2^--N, NO_3^--N, and TN concentrations in WD had significant positive correlations with the abundances of nitrogen cycling genes. Among them, the TAN concentration had significant positive correlations with the abundances of *napA*, *narG*, *nirK*, and *ureC*; the NO_2^--N concentration had significant positive correlations with the *amoA*, *napA*, *narG*, *nirK*, *nirS*, and *ureC*; the NO_3^--N concentration had significant positive correlations with *amoA*, *napA*, *narG*, *nirK*, and *ureC*; and the TN concentration had significant positive correlations with *napA*, *narG*, and *ureC* ($p < 0.05$). TOC, C/N, and pH were not significantly correlated with the abundances of nitrogen cycling genes ($p > 0.05$). T had significant negative correlations with the abundances of *amoA*, *napA*, *narG*, *nirK*, and *ureC*, and DO also had significant negative correlations with *napA*, *narG*, *nirK*, and *ureC* ($p < 0.05$).

Table 2. Pearson's correlation analysis between nitrogen cycling gene abundances and environmental factors in WD.

	TAN	NO_2^--N	NO_3^--N	TN	TOC	C/N	pH	T	DO
amoA	0.40	0.47 *	0.47 *	0.31	−0.05	0.04	0.11	−0.53 *	−0.43
napA	0.52 *	0.55 *	0.64 **	0.53 *	0.00	−0.20	−0.27	−0.53 *	−0.45 *
narG	0.67 **	0.57 **	0.49 *	0.58 **	0.21	−0.17	−0.05	−0.60 **	−0.48 *
nxrB	0.32	0.35	0.20	0.36	0.13	−0.01	0.06	−0.43	−0.27
nirK	0.45 *	0.47 *	0.50 *	0.24	0.08	0.01	0.03	−0.51 *	−0.52 *
nirS	0.14	0.45 *	0.35	0.34	0.12	0.07	0.16	−0.53	−0.07
ureC	0.88 ***	0.81 ***	0.81 ***	0.72 ***	0.16	−0.21	−0.41	−0.81 ***	−0.80 ***

Note. The coefficients (r) are shown. Significance levels: *: *p* value < 0.05, **: *p* value < 0.01, and ***: *p* value < 0.001. The same below.

The correlation analysis of nitrogen cycling genes and environmental factors of CY is shown in Table 3. The TAN concentration had significant positive correlations with the abundances of *amoA*, *narG*, and *nirS* and significant negative correlations with *napA*, *nxrB*, and *nirK* ($p < 0.05$). Concentrations of NO_2^--N and NO_3^--N had a significant positive correlation with the abundance of *nxrB* ($p < 0.05$); the TN concentration had a significant positive correlation with *amoA* and significant negative correlations with *napA* and *nirK* ($p < 0.05$); TOC had significant positive correlations with the abundances of *nirK* and *ureC* ($p < 0.05$); and the C/N ratio was positively correlated with *napA* and negatively correlated with *ureC* ($p < 0.05$). Moreover, pH and *napA's* abundance also had a significantly positive correlation ($p < 0.05$). T had a significant positive correlation with the abundance of *ureC*, and DO had significant positive correlations with the abundances of *nxrB* and *nirK* ($p < 0.05$).

Table 3. Pearson's correlation analysis between the functional gene abundances and environmental factors in CY. Note: The coefficients (r) are shown in the table. Significance levels: *: $p < 0.05$, **: p value < 0.01, and ***: $p < 0.001$.

|	TAN	NO_2^--N	NO_3^--N	TN	TOC	C/N	pH	T	DO
amoA	0.46 *	0.10	0.38	0.4689 *	0.1595	−0.18	−0.36	−0.17	0.16
napA	−0.49 *	−0.27	−0.43	−0.7194 ***	−0.0835	0.52 *	0.68 **	−0.06	0.42
narG	0.63 **	−0.14	0.04	0.2706	0.2831	−0.15	−0.34	0.14	−0.28
nxrB	−0.54 *	0.48 *	0.51 *	−0.0282	−0.4055	−0.10	0.08	−0.27	0.57 **
nirK	−0.70 *	0.14	−0.01	−0.5115 *	−0.4825 *	0.25	0.26	−0.13	0.45 *
nirS	0.49 *	0.09	0.20	0.3513	0.2876	−0.21	−0.44	0.12	−0.31
ureC	0.07	−0.11	−0.09	0.0552	−0.5078 *	−0.46 *	−0.02	0.63 **	−0.21

3.10. Correlations between Dominant Bacterial Communities and Environmental Factors

The correlation analysis of water-dominant bacteria and environmental factors in the WD group is shown in Figure 9a–e. In WD1, *Flavobacteriaceae* had a significant positive correlation with TAN, and *Alteromonadaceae* had a significant positive correlation with NO_3^--N concentration ($p < 0.05$). In WD3, the abundances of *Flavobacteriaceae* and *Saprospiraceae* had significant positive correlations with the NO_2^--N concentration ($p < 0.05$). In WD5, the abundances of *Cyanobiaceae* and *Halieaceae* were significantly positively correlated with the NO_2^--N concentration ($p < 0.05$). In WD7, the abundances of *Cryomorphaceae* and *Microbacteriaceae* had significant positive correlations with the TAN concentration and TOC ($p < 0.05$). In WD9, the abundance of *Flavobacteriaceae* had a significant positive correlation with the NO_3^--N concentration and DO, and that of *f-37-13* had a significant positive correlation with the NO_3^--N concentration and pH ($p < 0.05$).

The correlation analysis of the water-dominant bacteria and environmental factors in the CY group is shown in Figure 10a–e. In CY3, the abundance of *Cyclobacteriaceae* had a significantly negative correlation with the NO_2^--N concentration. The abundance of the *NS9_marine_group* had a significantly positive correlation with the C/N ratio, and that of *norank_o__PeM15* was significantly positively correlated with DO ($p < 0.05$). In CY5, the abundance of *norank_o__PeM15* showed a significant positive correlation with the TAN concentration and T, and that of *Cyclobacteriaceae* showed a significant positive correlation with the C/N ratio ($p < 0.05$). In CY9, the abundances of *Rhodobacteraceae* showed a significant negative correlation with C/N, that of Flavobacteriaceae showed a significant positive correlation with DO, that of *Microbacteriaceae* showed a significant positive correlation with NO_2^--N, and that of *norank_o__PeM15* showed a significant positive correlation with NO_3^--N ($p < 0.05$).
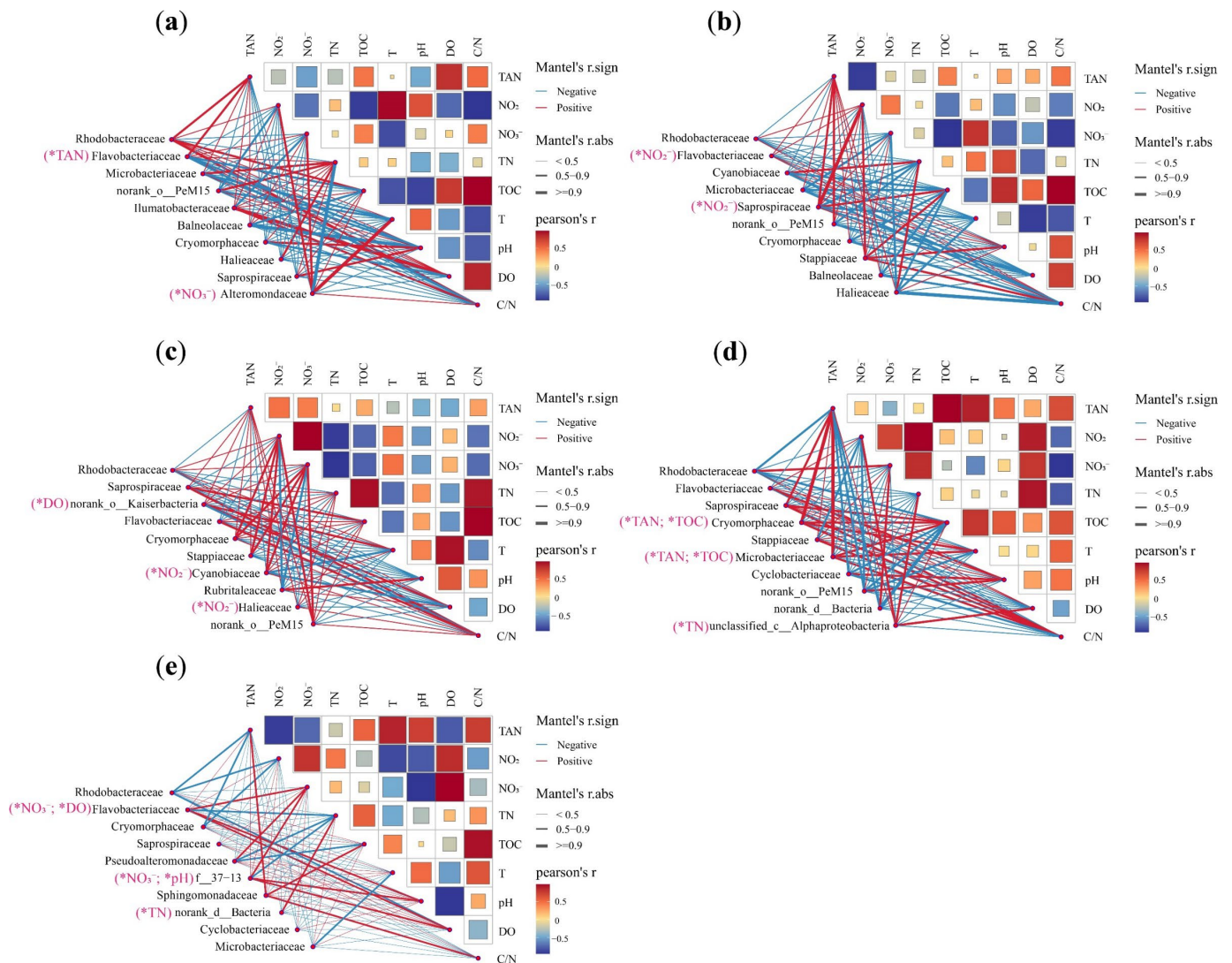
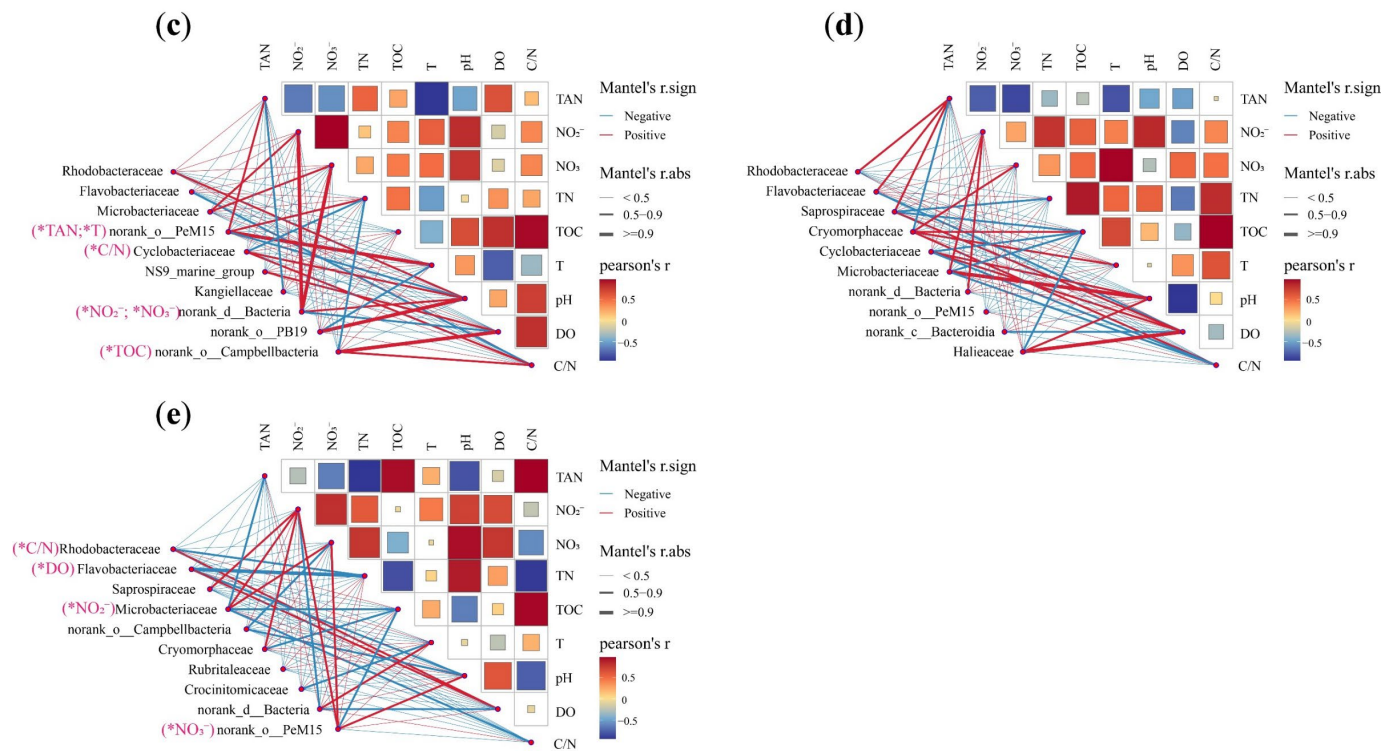**Figure 9.** Correlation analysis of water environmental factors and dominant bacteria in WD. (**a**): Week 1; (**b**): Week 3; (**c**): Week 5, (**d**): Week 7, (**e**): Week 9. Note: In the network diagram, the red line indicates a positive correlation and the blue line indicates a negative correlation. The thickness of the line indicates the degree of correlation. "*" indicates that there was a significant correlation between microbes and environmental factors ($p < 0.05$).
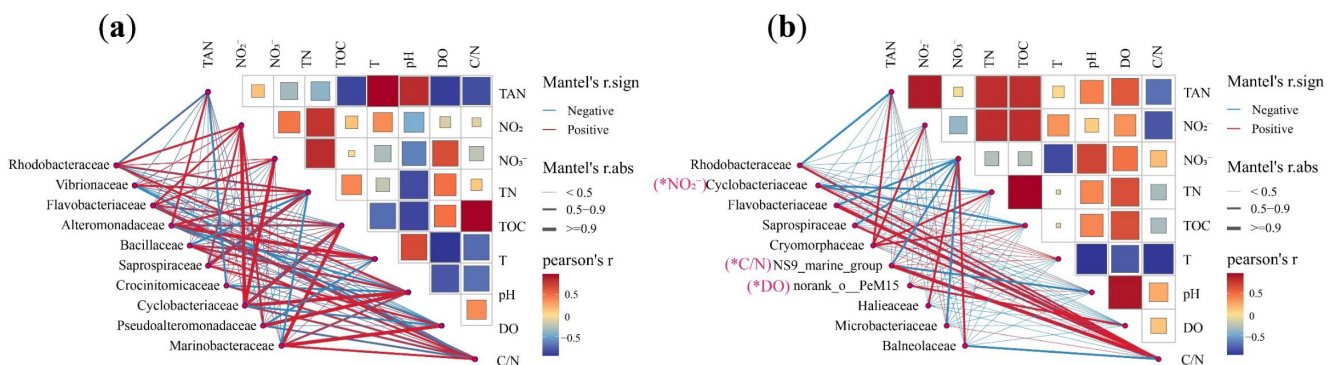
Figure 10. *Cont*.

Figure 10. Correlation analysis of water environmental factors, nitrogen cycling functional genes, and dominant bacteria in CY. (**a**): Week 1, (**b**): Week 3, (**c**): Week 5, (**d**): Week 7, (**e**): Week 9. "*" indicates that there was a significant correlation between microbes and environmental factors ($p < 0.05$).

4. Discussion

4.1. Diversity Indices of Bacterial Communities

The α-diversity of bacterial community reflects the species abundance, diversity, and functional potential of a community [27]. It is generally believed that communities with high α-diversity have better functions, can better resist external interference, and can maintain their stability [28,29]. As a measure of α-diversity, the ACE index reflects the individual number and species richness of species in a community. The Shannon index reflects the heterogeneity of the community and the evenness of the species distribution. In this study, the ACE and Shannon indices of the WD and CY groups both increased, indicating that the bacterial community of water in industrial farming systems became more stable with the progression of culture. According to the study of Li et al., the ACE and Shannon indices of bacterial communities in outdoor aquaculture water showed a decreasing trend with the progression of aquaculture [30], which was different from the trend of the corresponding indices in this study. This may be due to the differences in environmental conditions and management strategies between outdoor ponds and breeding plants.

The β-diversity reflects the differences between bacterial communities of different groups [31]. In this study, the WD1 to WD9 samples were dispersed, and there were significant differences among these groups. Except for CY1, the distributions of the samples in the CY group were similar, indicating that the change in water communities in CY was not significantly varied during culture. It is also the same as the message conveyed by the non-significant difference in α-diversity among CY groups. WD used natural seawater for farming, while CY is a mixture of seawater and groundwater. There were natural differences in bacterial species and diversity between the two aquaculture waters: *Cyanobiaceae*'s abundance was higher in the early stage of WD, while *Vibrionaceae* and *Alteromonadaceae* were higher in CY. The initial diversity and species of bacterial communities have a potential influence on the succession and development direction of the bacterial community [27].

The subsequent succession direction of the WD and CY bacterial communities in the water in the present study may be related to this difference.

In addition, in the first few weeks of culture, the dominant bacterial communities of WD and CY differed greatly (Figure S2a–c); however, as the culture progressed, the dominant bacterial families of WD and CY in the same period gradually approached each other (Figure S2d,e). At Weeks 7 and 9, the composition and relative abundance of the dominant bacteria were relatively similar. Management and feeding in aquaculture affect the bacterial community in the culture water [32,33]. The factors that led to similarity of the bacterial communities between the two water types in the later period of culture remain to be further explored.

4.2. Characteristics and Succession of Dominant Bacteria in the Bacterial Community

Microbes are the most important biological factors in the culture environment, and they are also affected by the environment [34–36]. In WD, the abundance of *Rhodobacteraceae* gradually increased, while that of *Flavobacteriaceae* remained stable. In the CY group, *Rhodobacteraceae* always maintained a high abundance, while the abundance of *Flavobacteriaceae* showed a decreasing trend. Members of *Rhodobacteraceae* are complex and have many nutrient modes, and diverse trophic modes mean that *Rhodobacteraceae* can use various forms of organic matter [21,37]. *Flavobacteriaceae* can exploit complex organic matter in water, especially polysaccharides and proteins; decompose these substances; and release energy for growth and reproduction [21,38]. In this research, the abundances of *Rhodobacteraceae* and *Flavobacteriaceae* in the CY group almost exceeded 50% throughout the whole culture process. In the WD group, the percentage was slightly lower but not less than 22%. There was sufficient unused organic matter in the culture environment, which may be the reason for the high abundances of *Rhodobacteraceae* and *Flavobacteriaceae* in the culture water; their high abundances facilitate the decomposition of organic matter and release carbon and nitrogen that may be utilized by other microbes [21].

Saprospiraceae are dominant bacteria that often appear in water for farming [39]. In this research, *Saprospiraceae*'s abundance increased in both the WD and CY groups, especially in the middle and late stages of aquaculture. *Saprospiraceae* are mostly anaerobic or facultative anaerobic bacteria that can participate in multiple denitrification processes, such as nitrate reduction and nitrite reduction, due to functional genes such as *narG* and *nirB* [40]. *Saprospiraceae* also effectively remove ammonia nitrogen and total nitrogen [40,41]. In addition, *Saprospiraceae* can decompose complex organic compounds, such as proteins [42] and cellulose [43], providing a material basis for other reactions. Therefore, the increase in *Saprospiraceae* in the WD and CY groups may enhance the denitrification ability of water and promote the release of nitrogen compounds from the water in the form of N_2. On the other hand, it may also be conducive to the decomposition of organic matter in water.

Cryomorphaceae can participate in secondary production in the ocean [44] and decompose complex organic matter, which is related to the carbon and nitrogen cycles of water [45]. In the present study, *Cryomorphaceae*'s abundance in WD and CY tended to increase, which may be conducive to enhancing the DNRA process in water [46]. Notably, *Cryomorphaceae* in the WD and CY groups exhibited the same trend as that of the corresponding abundance of *Saprospiraceae*. Studies have shown that members of *Cryomorphaceae* need a high organic load to support their proliferation [44]. The abundances of both species exhibited the same trend, probably because *Saprospiraceae* activity provided the carbon needed for the proliferation of *Cryomorphaceae*. In addition, similar to *Saprospiraceae*, *Microbacteriaceae*, which rapidly declined in abundance from CY5 to CY7 (12.31% to 4.40%), also has the potential of heterotrophic nitrification and aerobic denitrification [47,48] and can decompose complex organics [49]. In both the WD and CY groups, the abundance of *Saprospiraceae* showed an opposite trend to that of *Microbacteriaceae*, and there may be a competitive relationship between them. The decrease in the abundance of *Microbacteriaceae* may be related to the increase in the abundance of *Saprospiraceae*.

Cyanobiaceae are bacterial markers of WD's early stage, whose abundance was 9.02% in WD3. Cyanobacteria are often considered potential nitrogen-fixing agents in the ocean, converting free nitrogen in the air into a form that can be directly used by organisms [17,50]. Furthermore, the results of functional prediction analysis showed that WD had strong photosynthetic capacity in the early stage. The bacterial community in WD3 had the highest photosynthetic abundance, which was approximately one-third of the chemosynthesis function, and was also consistent with the highest abundance of *Cyanobiaceae*. The prevalence of cyanobacteria provides more abundant nutrient channels for water and may be conducive to the succession of the bacterial community.

In the CY group, the relative abundances of *Vibrionaceae* and *Alteromonadaceae* were high in CY1 (22.83% for *Vibrionaceae* and 12.84% for *Alteromonadaceae*). Their abundances rapidly decreased after CY1, especially *Vibrionaceae*, whose abundance was almost zero. Although some *Vibrionaceae* species are pathogenic bacteria, members of this family can participate in the water–nitrogen cycle and remove various forms of nitrogen, such as ammonia nitrogen [51] and nitrate nitrogen [52], from the water. *Alteromonadaceae* species contain key genes involved in the nitrogen cycle, such as *amoA*, *napA*, *narG*, and *nirB*, and are functional bacteria capable of removing toxic nitrogen compounds such as nitrate [53]. Both *Vibrionaceae* and *Alteromonadaceae* have the potential capacity for nitrogen transformation. The result of the functional prediction analysis showed that the abundance of nitrate reduction function was extremely high in CY1 but rapidly decreased after CY1, which was consistent with the rapid decline in the abundances of *Vibrionaceae* and *Alteromonadaceae*. Therefore, *Vibrionaceae* and *Alteromonadaceae*, which had high relative abundances in CY1, may be involved in nitrate reduction.

The abundances of *Vibrionaceae* and *Alteromonadaceae* are associated with the C/N ratio in water. Outbreaks of *Vibrionaceae* and *Alteromonadaceae* often lead to a decrease in the C/N ratio in water [54,55]. We measured the C/N ratio of the water samples (Figure S3) and found that the C/N ratio was 16.3 in CY1 and decreased to 2.1 in CY3, and it remained low after CY3. Moreover, the abundances of *Vibrionaceae* and *Alteromonadaceae* also remained low, which was the same as the findings of Allers et al. [54].

4.3. Correlations between Nitrogen Cycling Genes and Environmental Factors

Gene abundance reflects the strength of the corresponding process and the speed of the reaction [56]. The results of gene abundance showed that functional gene abundance changed significantly during different culture stages, which may be related to changes in environmental factors during the culture process [34,57]. The *ureC* and *amoA* genes participate in the decomposition of nitrogen-containing particulate organic matter and the oxidation of ammonia nitrogen, respectively [12], which are related to the production of inorganic nitrogen compounds in water and the consumption of ammonia nitrogen. The *amoA* gene in the WD group increased in Weeks 5–7, and *ureC* first decreased and then increased in Weeks 5–7, which indicated that the consumption of ammonia nitrogen accelerated in Weeks 5–7 and that production slowed. During Weeks 7–9, the generation rate accelerated. The actual changes in ammonia nitrogen concentrations in the WD group at Weeks 7–9 (Figure S4) were also consistent with the trend exhibited by the changes in gene abundance. There was a synchronous relationship between the *amoA* and *ureC* genes and changes in the reaction rate and concentration of ammonia nitrogen, which was also consistent with the positive correlation between *ureC* and TAN concentrations in the WD group in this study.

The *nxrB* gene is a key gene involved in nitrite oxidation and works with *amoA* to complete the nitrification reaction [25]. In this study, *nxrB* in WD and CY exhibited a synergistic trend with that of *amoA*, which might be caused by the synergistic changes in ammonia-oxidizing bacteria and nitrite-oxidizing bacteria [58]. The *narG*, *nirS*, and *nirK* genes are key genes connected with the denitrification process; *narG* is involved in the dissimilar reduction of nitrate [59], and *nirS* and *nirK* are involved in the reduction of nitrite [60]. The abundance of *nirK* in both the WD and CY groups was over ten times

higher than that of *nirS*, which means *nirK* was dominant in the nitrate reduction process in the culture environment [61]. The correlation analysis also indicated that the correlation between *nirK* and nitrogen-containing compounds was stronger than that between *nirS* and those compounds. Denitrification is a highly modular process, with almost all stages being performed by different microbes [62], but not all bacterial products can be denitrified.

Studies have shown that denitrification with *nirK* participation is more difficult to complete the full reaction process than that with *nirS* participation, and the production of N$_2$O increases [61], which may have adverse effects on the environment. *napA* is a key gene in the DNRA process. It reduces nitrate and eventually generates ammonia nitrogen in the reaction, which can reduce the loss of nitrogen in water [63]. In both the WD and CY groups, the abundance of *napA* was relatively low and remained at 10^4 copies/mL, which was much lower than that of *narG*, for most of the culture process. These findings indicate that the intensity of denitrification in aquaculture water was greater than that of DNRA and that *narG* was the main gene involved in nitrate reduction. In addition to nitrogen compounds, T and DO were significantly negatively correlated with many functional genes. T and DO are important environmental factors of aquaculture water, and their impact on water function cannot be ignored [13,64].

4.4. Correlations between Bacterial Communities and Environmental Factors

Farming activities can often cause changes in environmental conditions, such as the C/N ratio, which is generally indicative of detritus and bacterial abundance. Changes in microbes, as the carriers of functional genes, are bound to cause fluctuations in the abundances of functional genes [57]. Correlation analysis between bacterial communities and environmental factors revealed that the dominant bacteria, for example, *Flavobacteriaceae*, *Cryomorphaceae*, *Saprospiraceae*, *Microbacteriaceae*, *Cyanobiaceae*, and *Halieaceae*, were significantly correlated with nitrogen compounds during the culture process. Previous studies have shown that *Flavobacteriaceae* species have nitrogen cycling genes such as *nirK*, which are related to nitrite transformation in water [21]. *Saprospiraceae* species have various functions as they are either aerobic or facultative anaerobic nitrifying bacteria and anaerobic denitrifying bacteria and are the main force in activated sludge biological nitrogen removal equipment [65,66]. In addition, the bacteria in the family *Microbacteriaceae* can perform heterotrophic nitrification and aerobic denitrification and can form anaerobic vacuoles in an aerobic environment to promote the progression of several anaerobic processes [47]. *Halieaceae* have the *napAB* and *nirBD* genes and have the potential to participate in DNRA processes [67]. These findings agree with the conclusions of the correlation analysis in this study, which indicate that *Flavobacteriaceae*, *Cryomorphaceae*, *Saprospiraceae*, *Microbacteriaceae*, *Cyanobiaceae*, and *Halieaceae* may be the key microbes affecting the concentrations of TAN and NO$_2$$^-$-N in the water.

5. Conclusions

At present, industrial farming is one of the main farming systems used for *L. vannamei*, and it is also the main direction of development in the future. In this research, the water of two typical *L. vannamei* aquaculture ponds was collected, the environmental indicators of the water were measured, and the characteristics of the bacterial community and the relationships between bacterial abundance, nitrogen cycling genes, and environmental factors were analyzed. According to the results, there were photosynthetic cyanobacteria in the WD water, and the bacterial community of the CY water had strong denitrification potential in the early stage of culture. The diversity and abundance of bacterial communities in the WD and CY water samples showed different trends. Changes in ammonia nitrogen and nitrate nitrogen in water may be caused by *Flavobacteriaceae*, *Saprospiraceae*, *Cryomorphaceae*, *Cyanobiaceae*, *Halieaceae*, and *Cyclobacteriaceae*. Changes in water environment factors, such as nitrogen concentration, DO concentration, and T, may also lead to the changes in the bacterial community. Our research explored the bacterial groups that play key roles in the nitrogen cycle, deepening our understanding of the rapid increase in ammonia nitrogen

and nitrite concentrations in industrial farming systems and providing a theoretical basis for solutions.

References

1. FAO. *The State of World Fisheries and Aquaculture 2022. Towards Blue Transformation*; FAO: Rome, Italy, 2022. [CrossRef]
2. Wang, D.; Wu, F.X.; Song, D.D.; Gao, H.Q. *China Fisheries Statistic Yearbook 2023*; China Agriculture Press: Beijing, China, 2023.
3. Gao, D.Z.; Liu, M.; Hou, L.J.; Derrick, Y.F.L.; Wang, W.Q.; Li, X.F.; Zeng, A.Y.; Zheng, Y.L.; Han, P.; Yang, Y.; et al. Effects of shrimp-aquaculture reclamation on sediment nitrate dissimilatory reduction processes in a coastal wetland of southeastern China. *Environ. Pollut.* **2019**, *255*, 113219. [CrossRef] [PubMed]
4. Garcon, D.P.; Fabri, L.M.; Moraes, C.M.; Costa, M.I.C.; Freitas, R.S.; McNamara, J.C.; Leone, F.A. Effects of ammonia on gill (Na$^+$, K$^+$)-ATPase kinetics in a hololimnetic population of the Amazon River shrimp *Macrobrachium amazonicum*. *Aquat. Toxicol.* **2022**, *246*, 106144. [CrossRef] [PubMed]
5. Parvathy, A.J.; Das, B.C.; Jifiriya, M.J.; Varghese, T.; Pillai, D.; Kumar, V.J.R. Ammonia induced toxico-physiological responses in fish and management interventions. *Rev. Aquac.* **2023**, *15*, 452–479. [CrossRef]
6. Li, Y.D.; Zhou, F.L.; Huang, J.H.; Yang, L.S.; Jiang, S.; Yang, Q.B.; He, J.G.; Jiang, S.G. Transcriptome reveals involvement of immune defense, oxidative imbalance, and apoptosis in ammonia-stress response of the black tiger shrimp (*Penaeus monodon*). *Fish Shellfish. Immunol.* **2018**, *83*, 162–170. [CrossRef] [PubMed]
7. Liang, Z.X.; Liu, R.; Zhao, D.P.; Wang, L.L.; Sun, M.Z.; Wang, M.Q.; Song, L.S. Ammonia exposure induces oxidative stress, endoplasmic reticulum stress and apoptosis in hepatopancreas of pacific white shrimp (*Litopenaeus vannamei*). *Fish Shellfish. Immunol.* **2016**, *54*, 523–528. [CrossRef]
8. Zhao, M.M.; Yao, D.F.; Li, S.K.; Zhang, Y.L.; Aweya, J.J. Effects of ammonia on shrimp physiology and immunity: A review. *Rev. Aquac.* **2020**, *12*, 2194–2211. [CrossRef]
9. Romano, N.; Zeng, C.S. Toxic effects of ammonia, nitrite, and nitrate to decapod crustaceans: A review on factors influencing their toxicity, physiological consequences, and coping mechanisms. *Rev. Fish. Sci.* **2013**, *21*, 1–21. [CrossRef]
10. Liang, Q.J.; Li, A.; Wu, L.T.; Zhang, Y.; Han, T.; Liu, X. scRNA-seq analysis reveals toxicity mechanisms in shrimp hemocytes subjected to nitrite stress. *Chemosphere* **2023**, *316*, 137853. [CrossRef] [PubMed]
11. Tseng, I.T.; Chen, J.C. The immune response of white shrimp *Litopenaeus vannamei* and its susceptibility to *Vibrio alginolyticus* under nitrite stress. *Fish Shellfish. Immunol.* **2004**, *17*, 325–333. [CrossRef]

12. Kuypers, M.M.M.; Marchant, H.K.; Kartal, B. The microbial nitrogen-cycling network. *Nat. Rev. Microbiol.* **2018**, *16*, 263–276. [CrossRef]

13. Braker, G.; Schwarz, J.; Conrad, R. Influence of temperature on the composition and activity of denitrifying soil communities. *FEMS Microbiol. Ecol.* **2010**, *73*, 134–148. [CrossRef] [PubMed]

14. Bao, P.; Wang, S.; Gao, Y.; Ma, B.; Zhang, Q.; Peng, Y. Effect of dissolved oxygen on microbial community of nitrify activated sludge based on high-throughput sequencing technology. *J. Beijing Univ. Technol.* **2017**, *43*, 801–808. [CrossRef]

15. Park, M.; Kim, J.M.; Lee, T.; Oh, Y.K.; Nguyen, V.; Cho, S. Correlation of microbial community with salinity and nitrogen removal in an anammox-based denitrification system. *Chemosphere* **2021**, *263*, 128340. [CrossRef] [PubMed]

16. Wu, X.T.; Sun, Y.; Deng, L.T.; Meng, Q.X.; Jiang, X.; Bello, A.; Sheng, S.Y.; Han, Y.; Zhu, H.F.; Xu, X.H. Insight to key diazotrophic community during composting of dairy manure with biochar and its role in nitrogen transformation. *Waste Manag.* **2020**, *105*, 190–197. [CrossRef] [PubMed]

17. Thompson, A.W.; Foster, R.A.; Krupke, A.; Carter, B.J.; Musat, N.; Vaulot, D.; Kuypers, M.M.M.; Zehr, J.P. Unicellular Cyanobacterium symbiotic with a single-celled eukaryotic alga. *Science* **2012**, *337*, 1546–1550. [CrossRef] [PubMed]

18. Malm, S.; Tiffert, Y.; Micklinghoff, J.; Schultze, S.; Joost, I.; Weber, I.; Horst, S.; Ackermann, B.; Schmidt, M.; Wohlleben, W.; et al. The roles of the nitrate reductase NarGHJI, the nitrite reductase NirBD and the response regulator GlnR in nitrate assimilation of *Mycobacterium tuberculosis. Microbiology* **2009**, *155*, 1332–1339. [CrossRef] [PubMed]

19. Chen, Z.; Chang, Z.; Qiao, L.; Wang, J.; Li, J. Nitrogen removal performance and microbial diversity of bioreactor packed with cellulosic carriers in recirculating aquaculture system. *Int. Biodeterior. Biodegrad.* **2021**, *157*, 105157. [CrossRef]

20. Chen, C.T.; Wang, F.; Ren, Z.W.; Wang, X.C.; Shan, H.W. Influencing factors on nitrite removal by bagasse biofloss and the succession of attached bacterial communities. *J. Water Process. Eng.* **2024**, *59*, 105057. [CrossRef]

21. Hu, D.; Zeng, J.; Wang, L.; Shao, Z.; Zhao, R. Core microbiome involved in nitrite removal in shrimp culture ponds. *Aquac. Res.* **2022**, *53*, 1663–1675. [CrossRef]

22. Wang, Z.J.; Feng, K.; Wei, Z.Y.; Wu, Y.N.; Isobe, K.; Senoo, K.; Peng, X.; Wang, D.R.; He, Q.; Du, X.F.; et al. Evaluation and redesign of the primers for detecting nitrogen cycling genes in environments. *Methods Ecol. Evol.* **2022**, *13*, 1976–1989. [CrossRef]

23. Dong, L.H.; Meng, Y.; Wang, J.; Liu, Y.Y. Evaluation of droplet digital PCR for characterizing plasmid reference material used for quantifying ammonia oxidizers and denitrifiers. *Anal. Bioanal. Chem.* **2014**, *406*, 1701–1712. [CrossRef] [PubMed]

24. Chen, Z.; Luo, X.Q.; Hu, R.G.; Wu, M.N.; Wu, J.S.; Wei, W.X. Impact of long-term fertilization on the composition of denitrifier communities based on nitrite reductase analyses in a paddy soil. *Microb. Ecol.* **2010**, *60*, 850–861. [CrossRef] [PubMed]

25. Keeley, R.F.; Rodriguez-Gonzalez, L.; Class, U.; Briggs, G.E.; Frazier, V.E.; Mancera, P.A.; Manzer, H.S.; Ergas, S.J.; Scott, K.M. Degenerate PCR primers for assays to track steps of nitrogen metabolism by taxonomically diverse microorganisms in a variety of environments. *J. Microbiol. Methods* **2020**, *175*, 105990. [CrossRef] [PubMed]

26. Khanal, A.; Lee, J.H. Functional diversity and abundance of nitrogen cycle-related genes in paddy soil. *Appl. Biol. Chem.* **2020**, *63*, 17. [CrossRef]

27. Xun, W.B.; Li, W.; Xiong, W.; Ren, Y.; Liu, Y.P.; Miao, Y.Z.; Xu, Z.H.; Zhang, N.; Shen, Q.R.; Zhang, R.F. Diversity-triggered deterministic bacterial assembly constrains community functions. *Nat. Commun.* **2019**, *10*, 3833. [CrossRef] [PubMed]

28. Ptacnik, R.; Solimini, A.G.; Andersen, T.; Tamminen, T.; Brettum, P.; Lepistö, L.; Willén, E.; Rekolainen, S. Diversity predicts stability and resource use efficiency in natural phytoplankton communities. *Proc. Natl. Acad. Sci. USA* **2008**, *105*, 5134–5138. [CrossRef]

29. Shanahan, F. Probiotics in Perspective. *Gastroenterology* **2010**, *139*, 1808–1812. [CrossRef] [PubMed]

30. Li, J.N.; Liu, G.B.; Liu, Q.; Wang, F.; Shan, H.W.; Xie, Y.C.; Li, C.J. Microbial community dynamics and its correlation with environmental factors in the water of polyculture ponds containing *Penaeus japonicus*, *Portunus trituberculatus* and *Sinonovacula constricta. Aquat. Ecol.* **2023**, *57*, 263–279. [CrossRef]

31. Ingerslev, H.C.; Jorgensen, L.V.; Strube, M.L.; Larsen, N.; Dalsgaard, I.; Boye, M.; Madsen, L. The development of the gut microbiota in rainbow trout (*Oncorhynchus mykiss*) is affected by first feeding and diet type. *Aquaculture* **2014**, *424*, 24–34. [CrossRef]

32. Dunne, A.; Carvalho, S.; Morán, X.A.G.; Calleja, M.L.; Jones, B. Localized effects of offshore aquaculture on water quality in a tropical sea. *Mar. Pollut. Bull.* **2021**, *171*, 112732. [CrossRef]

33. Zhao, R.X.; Symonds, J.E.; Walker, S.P.; Steiner, K.; Carter, C.G.; Bowman, J.P.; Nowak, B.F. Effects of feed ration and temperature on Chinook salmon (*Oncorhynchus tshawytscha*) microbiota in freshwater recirculating aquaculture systems. *Aquaculture* **2021**, *543*, 736965. [CrossRef]

34. Gao, Y.; Ding, J.J.; Yuan, M.T.; Chiariello, N.; Docherty, K.; Field, C.; Gao, Q.; Gu, B.H.; Gutknecht, J.; Hungate, B.A.; et al. Long-term warming in a Mediterranean-type grassland affects soil bacterial functional potential but not bacterial taxonomic composition. *Npj Biofilms Microbomes* **2021**, *7*, 17. [CrossRef] [PubMed]

35. Louca, S.; Parfrey, L.W.; Doebeli, M. Decoupling function and taxonomy in the global ocean microbiome. *Science* **2016**, *353*, 1272–1277. [CrossRef] [PubMed]

36. Liu, Q.; Lei, X.J.; Li, J.N.; Chu, L.X.; Wang, F.; Shan, H.W.; Hu, F.G. Microbial communities and nitrogen cycling in *Litopenaeus vannamei* and *Mercenaria mercenaria* polyculture ponds. *Aquacult. Rep.* **2023**, *33*, 101769. [CrossRef]

37. Moschos, S.; Kormas, K.A.; Karayanni, H. Prokaryotic diversity in marine and freshwater recirculating aquaculture systems. *Rev. Aquac.* **2022**, *14*, 1861–1886. [CrossRef]

38. Silva, T.; Vieira, E.; Lopes, A.R.; Nunes, O.C.; Fonseca, A.; Saraiva, I.; Boaventura, R.A.R.; Vilar, V.J.P. How the performance of a biological pre-oxidation step can affect a downstream photo-Fenton process on the remediation of mature landfill leachates: Assessment of kinetic parameters and characterization of the bacterial communities. *Sep. Purif. Technol.* **2017**, *175*, 274–286. [CrossRef]

39. Califano, G.; Kwantes, M.; Abreu, M.H.; Costa, R.; Wichard, T. Cultivating the macroalgal holobiont: Effects of integrated multi-trophic aquaculture on the microbiome of *Ulva rigida* (Chlorophyta). *Front. Mar. Sci.* **2020**, *7*, 52. [CrossRef]

40. Zhang, L.F.; Fu, G.K.; Zhang, Z. Simultaneous nutrient and carbon removal and electricity generation in self-buffered biocathode microbial fuel cell for high-salinity mustard tuber wastewater treatment. *Bioresour. Technol.* **2019**, *272*, 105–113. [CrossRef] [PubMed]

41. Zhou, G.W.; Zhou, Y.H.; Zhou, G.Q.; Lu, L.; Wan, X.K.; Shi, H.X. Assessment of a novel overflow-type electrochemical membrane bioreactor (EMBR) for wastewater treatment, energy recovery and membrane fouling mitigation. *Bioresour. Technol.* **2015**, *196*, 648–655. [CrossRef]

42. Jiang, X.; Ma, H.; Zhao, Q.L.; Yang, J.; Xin, C.Y.; Chen, B.C. Bacterial communities in paddy soil and ditch sediment under rice-crab co-culture system. *AMB Express* **2021**, *11*, 163. [CrossRef]

43. Tarnecki, A.M.; Levi, N.J.; Resley, M.; Main, K. Effect of copper sulfate on the external microbiota of adult common snook (*Centropomus undecimalis*). *Anim. Microbiome* **2021**, *3*, 21. [CrossRef] [PubMed]

44. Califano, G.; Castanho, S.; Soares, F.; Ribeiro, L.; Cox, C.J.; Mata, L.; Costa, R. Molecular taxonomic profiling of bacterial communities in a gilthead seabream (*Sparus aurata*) hatchery. *Front. Microbiol.* **2017**, *8*, 204. [CrossRef] [PubMed]

45. Han, F.; Zhang, M.R.; Liu, Z.; Han, Y.F.; Li, Q.; Zhou, W.Z. Enhancing robustness of halophilic aerobic granule sludge by granular activated carbon at decreasing temperature. *Chemosphere* **2022**, *292*, 133507. [CrossRef] [PubMed]

46. Kong, S.; Chen, Z.; Ghonimy, A.; Zhao, F.Z.; Li, J. Effects of *Penaeus japonicus* stocking density on water quality and bacterial community structure in water in an integrated multi-trophic aquaculture (IMTA) system. *Fish. Sci.* **2023**, *90*, 75–91. [CrossRef]

47. Janka, E.; Pathak, S.; Rasti, A.; Gyawali, S.; Wang, S. Simultaneous heterotrophic nitrification and aerobic denitrification of water after sludge dewatering in two sequential moving bed biofilm reactors (MBBR). *Int. J. Environ. Res. Public Health* **2022**, *19*, 1841. [CrossRef] [PubMed]

48. Zheng, L.; Xing, Y.Z.; Ding, A.Z.; Sun, S.Q.; Cheng, H.G.; Bian, Z.Y.; Yang, K.; Wang, S.R.; Zhu, G.B. Brownification of freshwater promotes nitrogen-cycling microorganism growth following terrestrial material increase and ultraviolet radiation reduction. *Sci. Total Environ.* **2022**, *853*, 158556. [CrossRef] [PubMed]

49. Deng, Y.Q.; Mao, C.; Chen, H.X.; Wang, B.T.; Cheng, C.H.; Ma, H.L.; Guo, Z.X.; Feng, J.; Su, Y.L. Shifts in pond water bacterial communities are associated with the health status of sea bass (*Lateolabrax maculatus*). *Ecol. Indic.* **2021**, *127*, 107775. [CrossRef]

50. Zhou, Y.; Anwar, M.N.; Guo, B.; Huang, W.Y.; Liu, Y. Response of antibiotic resistance genes and microbial niches to dissolved oxygen in an oxygen-based membrane biofilm reactor during greywater treatment. *Sci. Total Environ.* **2022**, *833*, 155062. [CrossRef] [PubMed]

51. Liu, X.; Wang, Q.K.; Li, L.X.; Sun, X.L.; Lv, A.J.; Chen, C.X. Characterization of aerobic denitrification genome sequencing of *Vibrio parahaemolyticus* strain HA2 from recirculating mariculture system in China. *Aquaculture* **2020**, *526*, 735295. [CrossRef]

52. Ren, J.L.; Ma, H.J.; Liu, Y.; Ruan, Y.J.; Wei, C.Z.; Song, J.; Wu, Y.H.; Han, R. Characterization of a novel marine aerobic denitrifier *Vibrio* spp. AD2 for efficient nitrate reduction without nitrite accumulation. *Environ. Sci. Pollut. Res.* **2021**, *28*, 30807–30820. [CrossRef]

53. Xia, X.M.; Zheng, Q.; Leung, S.K.; Wang, Y.; Lee, P.Y.; Jing, H.M.; Jiao, N.Z.; Liu, H.B. Distinct metabolic strategies of the dominant heterotrophic bacterial groups associated with marine Synechococcus. *Sci. Total Environ.* **2021**, *798*, 149208. [CrossRef] [PubMed]

54. Allers, E.; Niesner, C.; Wild, C.; Pernthaler, J. Microbes enriched in seawater after addition of coral mucus. *Appl. Environ. Microbiol.* **2008**, *74*, 3274–3278. [CrossRef] [PubMed]

55. Guo, H.P.; Huang, L.; Hu, S.T.; Chen, C.; Huang, X.L.; Liu, W.; Wang, S.P.; Zhu, Y.Y.; Zhao, Y.J.; Zhang, D.M. Effects of carbon/nitrogen ratio on growth, intestinal microbiota and metabolome of shrimp (*Litopenaeus vannamei*). *Front. Microbiol.* **2020**, *11*, 652. [CrossRef]

56. Smith, C.J.; Dong, L.F.; Wilson, J.; Stott, A.; Osborn, A.M.; Nedwell, D.B. Seasonal variation in denitrification and dissimilatory nitrate reduction to ammonia process rates and corresponding key functional genes along an estuarine nitrate gradient. *Front. Microbiol.* **2015**, *6*, 542. [CrossRef] [PubMed]

57. Krishnani, K.K. Detection and diversity of nitrifying and denitrifying functional genes in coastal aquaculture. *Aquaculture* **2010**, *302*, 57–70. [CrossRef]

58. Huang, M.L.; Wang, Z.; Qi, R. Enhancement of the complete autotrophic nitrogen removal over nitrite process in a modified single-stage subsurface vertical flow constructed wetland: Effect of saturated zone depth. *Bioresour. Technol.* **2017**, *233*, 191–199. [CrossRef]

59. Nie, M.; Li, Z. Bioprocess of nitrite accumulation in water—A review. *Chin. J. Biotechnol.* **2020**, *36*, 1493–1503. [CrossRef] [PubMed]

60. Braker, G.; Zhou, J.Z.; Wu, L.Y.; Devol, A.H.; Tiedje, J.M. Nitrite reductase genes (*nirK* and *nirS*) as functional markers to investigate diversity of denitrifying bacteria in Pacific northwest marine sediment communities. *Appl. Environ. Microbiol.* **2000**, *66*, 2096–2104. [CrossRef]

61. Xiong, J.P.; Ma, S.S.; He, X.Q.; Han, L.J.; Huang, G.Q. Nitrogen transformation and dynamic changes in related functional genes during functional-membrane covered aerobic composting. *Bioresour. Technol.* **2021**, *332*, 125087. [CrossRef]

62. Graf, D.R.H.; Jones, C.M.; Hallin, S. Intergenomic comparisons highlight modularity of the denitrification pathway and underpin the importance of community structure for N$_2$O emissions. *PLoS ONE* **2014**, *9*, e114118. [CrossRef]

63. Wu, X.J.; Peng, J.J.; Liu, P.F.; Bei, Q.C.; Rensing, C.; Li, Y.; Yuan, H.M.; Liesack, W.; Zhang, F.S.; Cui, Z.L. Metagenomic insights into nitrogen and phosphorus cycling at the soil aggregate scale driven by organic material amendments. *Sci. Total Environ.* **2021**, *785*, 147329. [CrossRef] [PubMed]

64. Jiang, X.Y.; Liu, C.Q.; Cai, J.; Hu, Y.; Shao, K.Q.; Tang, X.M.; Gong, Y.; Yao, X.L.; Xu, Q.J.; Gao, G. Relationships between environmental factors and N-cycling microbes reveal the indirect effect of further eutrophication on denitrification and DNRA in shallow lakes. *Water Res.* **2023**, *245*, 120572. [CrossRef] [PubMed]

65. Chen, Z.R.; Lei, X.Q.; Lai, Q.L.; Li, Y.; Zhang, B.Z.; Zhang, J.Y.; Zhang, H.J.; Yang, L.X.; Zheng, W.; Tian, Y.; et al. *Phaeodactylibacter xiamenensis* gen. nov., sp nov., a member of the family *Saprospiraceae* isolated from the marine alga *Phaeodactylum tricornutum. Int. J. Syst. Evol. Microbiol.* **2014**, *64*, 3496–3502. [CrossRef] [PubMed]

66. Tang, Y.P.; Wang, R.X.; Tan, L.Q.; Guo, L.; Duan, Y.F.; Yang, L.S.; Jiang, S.G.; Zhou, F.L.; Jiang, S.; Huang, J.H. Effects of live microalgae and algae powder on microbial community, survival, metamorphosis and digestive enzyme activity of *Penaeus monodon* larvae at different growth stages. *Aquaculture* **2020**, *526*, 735344. [CrossRef]

67. Li, S.H.; Kang, I.; Cho, J.C. Metabolic versatility of the family halieaceae revealed by the genomics of novel cultured isolates. *Microbiol. Spectr.* **2023**, *11*, e0387922. [CrossRef]